

Supplemental Material: Particle-Hole Transformation in Strongly-Doped Iron-Based Superconductors

Jose P. Rodriguez

Department of Physics and Astronomy,

California State University, Los Angeles, California 90032.

I. SCHWINGER-BOSON-SLAVE-FERMION FORMULATION

The on-site-orbital energy cost U_0 in the two-orbital t - J model, Eq. (1) in the Communication, tends to infinity. The U_0 -infinity limit is enforced by (i) replacing the operator $c_{i,\alpha,s}^\dagger$ that creates a spin s electron at iron site i in $d\pm$ orbital α with the composite creation operator

$$\tilde{c}_{i,\alpha,s}^\dagger = \begin{cases} b_{i,\alpha,s}^\dagger f_{i,\alpha} & \text{at hole doping,} \\ b_{i,\alpha,s} f_{i,\alpha}^\dagger & \text{at electron doping.} \end{cases} \quad (\text{S1})$$

Likewise, the destruction operator $c_{i,\alpha,s}$ that appears in Eq. (1) of the Communication must be replaced with the composite destruction operator $\tilde{c}_{i,\alpha,s}$, which is simply the hermitian conjugate of (S1). Above, $b_{i,\alpha,\uparrow}$ and $b_{i,\alpha,\downarrow}$ are the destruction operators for a pair of Schwinger bosons, and $f_{i,\alpha}$ is the destruction operator for a spinless slave fermion. They (ii) satisfy the constraint

$$1 = b_{i,\alpha,\uparrow}^\dagger b_{i,\alpha,\uparrow} + b_{i,\alpha,\downarrow}^\dagger b_{i,\alpha,\downarrow} + f_{i,\alpha}^\dagger f_{i,\alpha} \quad (\text{S2})$$

at each site and orbital[S1, S2]. Notice by (S1) that the composite creation operator $\tilde{c}_{i,\alpha,s}^\dagger$ destroys a spin-1/2 moment and replaces it with a spin singlet in the case of electron doping about half filling, while it destroys an empty site-orbital and replaces it with a spin-1/2 moment in the case of hole doping about half filling.

At half filling, a spin-1/2 moment exists at each site-orbital, and no slave fermions exist by the constraint (S2). Many-Schwinger-boson wavefunctions can be treated in occupation space, in such case, which leads to spin-1/2 configurations on the square lattice of iron atoms with $d\pm$ orbitals[S3]. Figure S1 shows the exact spectrum of the resulting two-orbital Heisenberg model over a 4×4 lattice of iron atoms at a putative quantum critical point. The total spin along z is constrained to $\sum S_z = 0$, while translation symmetry and orbital-swap symmetry are exploited to block-diagonalize the Hamiltonian. Dashed lines in Fig.

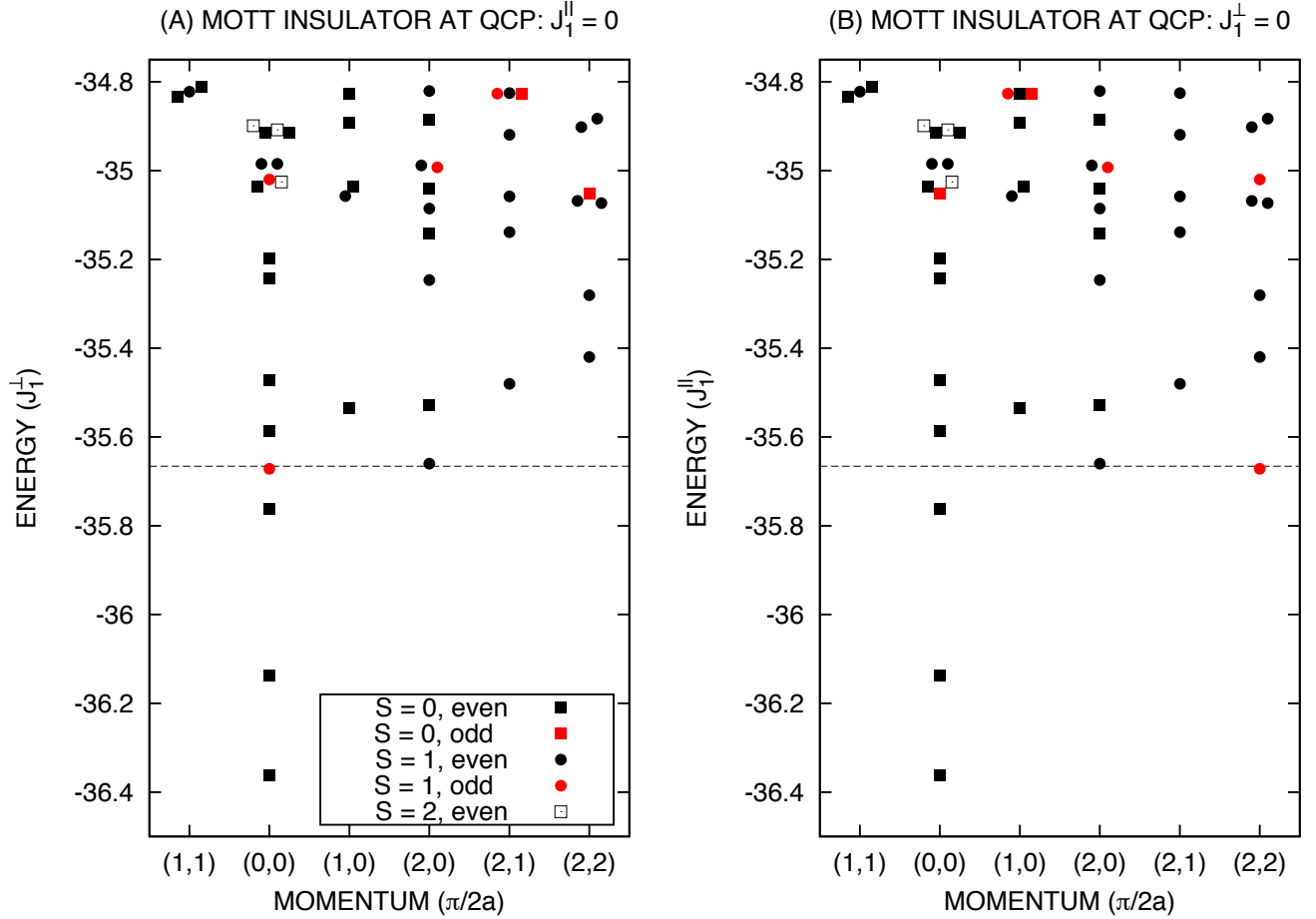


FIG. S1: Spectra for the two-orbital Heisenberg model over a periodic 4×4 lattice, with exchange coupling constants (a) $J_1^{\parallel} = 0$, $J_1^{\perp} > 0$, $J_2^{\parallel} = 0.3 J_1^{\perp} = J_2^{\perp}$. Model parameters transform to (b) $J_1^{\parallel} > 0$, $J_1^{\perp} = 0$, $J_2^{\parallel} = 0.3 J_1^{\parallel} = J_2^{\perp}$. And Hund coupling is set to the critical value $-J_0 = 1.35 J_1^{(\perp)\parallel}$. Black and red states are respectively even and odd under orbital swap.

S1 mark the degeneracy between the hidden-order spinwave and the spinwaves linked to commensurate spin-density-wave (cSDW) order. Heisenberg exchange coupling constants between Figs. S1a and S1b are related by the particle-hole transformation Eq. (5) in the Communication. Notice that states in Figs. S1a and Fig. S1b are paired following the previous particle-hole transformation, Eq. (3) in the Communication. In particular, states with even parity under orbital swap $P_{d,\bar{d}}$ have a twin in the adjacent spectrum. The twin state differs in momentum by $(\pi/a)(\hat{x} + \hat{y})$ for states with odd parity under $P_{d,\bar{d}}$, however[S3].

One slave fermion corresponds to one electron less than half filling in the case of hole doping and to one electron more than half filling in the case of electron doping by the previous Schwinger-boson-slave-fermion formulation, (S1) and (S2). Schwinger-boson degrees

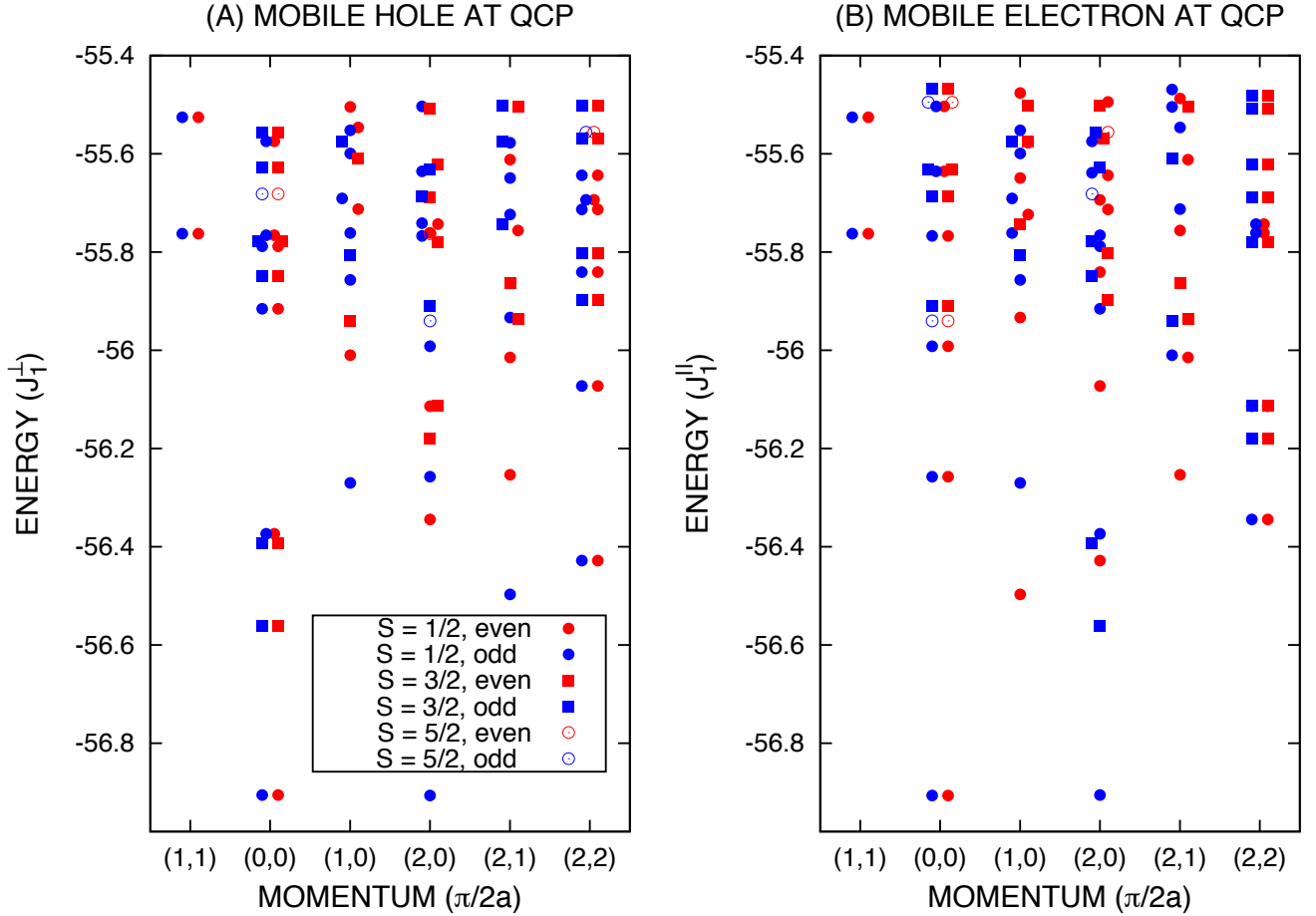


FIG. S2: Exact spectra of two-orbital t - J model, Eq. (1) in the Communication, over a periodic 4×4 lattice, with hopping parameters (a) $t_1^\parallel = -3J_1^\perp$, $t_1^\perp(\hat{x}) = -2J_1^\perp$, $t_1^\perp(\hat{y}) = +2J_1^\perp$, $t_2^\parallel = -J_1^\perp$, and $t_2^{d\pm, d\mp} = 0$ in the mobile-hole case (31 electrons). Hopping parameters transform to (b) $t_1^\parallel = 2J_1^\parallel$, $t_1^\perp(\hat{x}) = +3J_1^\parallel$, $t_1^\perp(\hat{y}) = -3J_1^\parallel$, $t_2^\parallel = -J_1^\parallel$, and $t_2^{d\pm, d\mp} = 0$ in the mobile-electron case (33 electrons). Heisenberg exchange coupling constants are given in the caption to Fig. S1, while Hund coupling is set to the critical value $-J_0 = 2.04J_1^{(\perp)\parallel}$.

of freedom can again be treated in occupation space, while the lone slave fermion can be treated in first quantization[S4, S5]. Figure S2 shows exact spectra for one mobile hole and for one mobile electron roaming over a 4×4 lattice of iron atoms obtained by employing such a description for the Hilbert space. Hund coupling $-J_0$ is tuned to a critical point at which the spin-1/2 ground states at zero 2D momentum and at cSDW momenta become degenerate. The mean-field result for the one-particle spectrum, Fig. 4 in the Communication, suggests that this degeneracy coincides with the quantum critical point (QCP) defined by the collapse of the spin gap at cSDW momenta [S3]: $\Delta_{cSDW} \rightarrow 0$. Any state in Fig. S2a

of parity $e^{ik_0} = \pm 1$ under orbital swap has a twin state of the same parity and at the same energy in Fig. S2b, but shifted by momentum \mathbf{Q}_{k_0} , where $\mathbf{Q}_0 = (\pi/a)\hat{\mathbf{y}}$ and $\mathbf{Q}_\pi = (\pi/a)\hat{\mathbf{x}}$.

Two slave fermions correspond to a mobile hole pair at hole doping, while they correspond to a mobile electron pair at electron doping. Again, the Schwinger-boson degrees of freedom can be treated in occupation space, while the pair of slave fermions can be treated in first quantization. In particular, fermion exchange symmetry can be enforced in first quantization[S6]. Figure 5 in the Communication shows the exact groundstate of a bound pair of mobile holes/electrons that roam over a 4×4 lattice, where such a scheme is employed to describe the Hilbert space.

II. ONE-ELECTRON SPECTRUM WITHIN MEAN FIELD APPROXIMATION

Consider the hole-doped case. At weak Hund coupling and in the presence of off-diagonal magnetic frustration, $J_1^\parallel < J_1^\perp$ and $J_2^\parallel, J_2^\perp > 0$, a hidden half metal with a background spin texture $\nearrow_{d-} \searrow_{d+}$ is expected at large electron spin s_0 for purely intra-orbital near-neighbor hopping of holes[S4, S5]. It results in degenerate Fermi surface hole pockets at the Brillouin zone center. A mean field treatment of the previous Schwinger-boson-slave-fermion formulation of the two-orbital t - J model at hole doping recovers this half metal groundstate at large electron spin s_0 [S4, S5]. The constraint (S2) is enforced on average over the bulk in such case.

The spin excitation spectrum predicted by the Schwinger-boson-slave-fermion mean field theory for the hidden half metal coincides with that predicted by the linear spin-wave approximation at half filling[S3]. (Cf. Figs. 1a and 1b in the Communication.) In particular, the Schwinger bosons disperse as $\omega_b(k_0, \mathbf{k}) = [\Omega_\parallel^2(\mathbf{k}) - \Omega_\perp^2(\mathbf{k})]^{1/2}$, where[S4, S5]

$$\begin{aligned}\Omega_\parallel(\mathbf{k}) &= s_0 \sum_{n=0,1,2} z_n J_n'^\perp - 4 \sum_{n=1,2} (s_0 J_n'^\parallel + t_n^\parallel x) [1 - \gamma_n(\mathbf{k})], \\ \Omega_\perp(\mathbf{k}) &= s_0 \sum_{n=0,1,2} z_n J_n'^\perp \gamma_n(\mathbf{k}).\end{aligned}$$

Above, $\gamma_0(\mathbf{k}) = 1$, $\gamma_1(\mathbf{k}) = \frac{1}{2}(\cos k_x a + \cos k_y a)$ and $\gamma_2(\mathbf{k}) = \frac{1}{2}(\cos k_+ a + \cos k_- a)$, with $k_\pm = k_x \pm k_y$, while $z_0 = 1$ and $z_1 = 4 = z_2$ are coordination numbers, and while $J' = (1 - x)^2 J$. Here, x denotes the concentration of mobile holes per iron site, per orbital. Hidden spinwaves ($k_0 = \pi$) disperse as ω_b , and they exhibit a Goldstone mode at $\mathbf{k} = 0$ with divergent spectral

weight. True spin waves ($k_0 = 0$) share the same dispersion, but with vanishing spectral weight at the Goldstone mode. They however have strong spectral weight at cSDW momenta $(\pi/a)\hat{\mathbf{x}}$ and $(\pi/a)\hat{\mathbf{y}}$, at which $\omega_b(0, \mathbf{k})$ shows a gap $\Delta_{cSDW} \propto \text{Re}(J_0 - J_{0c})^{1/2}$. It collapses to zero at a critical Hund coupling[S5]

$$-J_{0c} = 2(J_1^\perp - J_1^\parallel) - 4J_2^\parallel - (1-x)^{-2}s_0^{-1}2t_\parallel x, \quad (\text{S3})$$

where $t_\parallel = t_1^\parallel + 2t_2^\parallel$ is negative. Long-range cSDW order is expected at Hund coupling larger than $-J_{0c}$.

The one-particle propagator for the hidden half metal can also be computed within mean field theory[S4]. It shows a pole in frequency that corresponds to coherent hole propagation[S5], with a dispersion $\varepsilon_e(k_0, \mathbf{k}) = -4 \sum_{n=1,2} t_n^\parallel \gamma_n(\mathbf{k})$, and with a spectral weight $s_0\pi$. The imaginary part of the one-particle propagator also shows peaks that disperse in energy as $\varepsilon_e(k_0, 0) + \omega_b(k_0, \mathbf{k})$. They are intrinsically broad, but they become sharp near half filling[S6]. Figure 4a in the Communication shows the former coherent hole bands in addition to the latter (emergent) incoherent bands, which exhibit electron-type dispersion at cSDW wave numbers $(\pi/a)\hat{\mathbf{x}}$ and $(\pi/a)\hat{\mathbf{y}}$.

At electron doping, on the other hand, a hidden half metal with Néel order per $d \pm$ orbital is expected at weak Hund coupling for diagonal frustration $J_1^\parallel > J_1^\perp$ and $J_2^\parallel, J_2^\perp > 0$, with nearest neighbor inter-orbital electron hopping turned on: $t_1^\parallel = 0$, $t_1^\perp(\hat{\mathbf{x}}) > 0$, and $t_1^\perp(\hat{\mathbf{y}}) = -t_1^\perp(\hat{\mathbf{x}})$. Circular electron Fermi surface pockets exist at cSDW wavenumbers with orbital quantum numbers per Fig. 3b in the Communication. This hidden half metal of mobile electrons is related to the prior half metal state of mobile holes by the particle-hole transformation established in the Communication: Fig. 3 and Eqs. (3)-(5). Figure 4b in the Communication shows the coherent electron bands at cSDW wave numbers and the (emergent) incoherent hole bands at the center of the two-iron Brillouin zone that are obtained from a direct calculation of the one-electron propagator within the mean field approximation[S7].

[S1] C.L. Kane, P.A. Lee and N. Read, Phys. Rev. B **39**, 6880 (1989).

[S2] A. Auerbach and B. E. Larson, Phys. Rev. B **43**, 7800 (1991).

[S3] J.P. Rodriguez, Phys. Rev. B **82**, 014505 (2010).

- [S4] J.P. Rodriguez, M.A.N. Araujo, P.D. Sacramento, *Phys. Rev. B* **84**, 224504 (2011).
- [S5] J.P. Rodriguez, M.A.N. Araujo, P.D. Sacramento, *Eur. Phys. J. B* **87**, 163 (2014).
- [S6] J.P. Rodriguez, *J. Phys.: Condens. Matter* **28**, 375701 (2016).
- [S7] J.P. Rodriguez, *Phys. Rev. B* **95**, 134511 (2017).